MCP Papers in Press. Published on September 20, 2011 as Manuscript M111.009217

PROTEIN EXPRESSION REGULATION UNDER OXIDATIVE STRESS

Christine Vogel[1,2]*, Gustavo Monteiro Silva[1], Edward M. Marcotte[2]

[1] Center for Genomics and Systems Biology, New York University, New York, NY, USA

[2] Center for Systems and Synthetic Biology, Institute for Cellular and Molecular Biology, University of Texas at Austin, TX, USA

* Corresponding author: cvogel@nyu.edu

Document statistics: 5,100 words (incl. Methods), 3 figures, 2 tables

Keywords: translation regulation, oxidative stress, time course proteomics

ABSTRACT

Oxidative stress is known to affect both translation and protein turnover, but very few large-scale studies describe protein expression under stress. We measure protein concentrations in *Saccharomyces cerevisiae* over the course of two hours in response to a mild oxidative stress induced by diamide, providing detailed time-resolved information for 815 proteins, with additional data for another ~1,100 proteins. For the majority of proteins, we discover major differences between the global transcript and protein response. While mRNA levels often return to baseline one hour after treatment, protein concentrations continue to change. Integrating our data with features of translation and protein degradation, we are able to predict expression patterns for 41% of the proteins in the core dataset. Predictive features include, amongst others, targeting by RNA-binding proteins (Lhp1, Khd1), RNA secondary structures, RNA half-life, and translation efficiency under unperturbed conditions and in response to oxidative reagents – but not chaperone binding. We are able to both describe general dynamics of protein concentration changes, and to suggest possible regulatory mechanisms for individual proteins.

words: 169

Introduction

Cellular oxidative stress is characterized by an imbalance between reactive oxygen species (ROS) production and intracellular antioxidant defense, leading to potential damage (1). Low levels of intracellular ROS play a major role in redox signaling; but in high amounts ROS cause macromolecular damages. Protein oxidation can impair protein function, induce fragmentation, and promote promiscuous interactions that result in protein aggregation (2). The accumulation of intracellular protein aggregates may repress proteolysis, leading to cellular death by apoptosis (3). Maintaining low levels of protein oxidation is therefore a key part of balanced protein expression in the cell.

Oxidative stress plays a major role in a variety of human diseases, including atherosclerosis, diabetes (4), hypertension, neurological disorders as Alzheimer's (5) and Parkinson's disease (6), and cardiovascular disease (7). Moreover, impairment of the ubiquitin-proteasome system is associated with protein aggregation which is a hallmark of several neurodegenerative diseases (8, 9). Oxidatively modified proteins are also characteristic of cellular senescence and aging (10). The abnormal or prolonged production of oxidants is linked to DNA damage that results in gene mutations, altered gene expression and eventually cancer (11).

Baker's yeast has been successfully used as a model for neurodegenerative diseases and aging (12, 13), and its response pathways to oxidative stress are evolutionarily conserved with those in mammals (3). The yeast response to oxidative stress comprises extensive transcription regulation, for example through activation of transcription factors Yap1, Skn7, Msn2 and Msn4 (14). However, oxidative stress also impacts translation and protein degradation, affecting protein expression levels in addition to changes at the mRNA level. Translation and protein synthesis are generally down-regulated during oxidative stress, but specific RNAs are independently regulated in their translation depending on the type of stress (15, 16). For example, translation of the yeast Gcn2 protein kinase is inhibited, preventing phosphorylation of the eukaryotic translation initiation factor eIF2 (16). The reduced activity of the eIF2 complex results in decreased rates of translation initiation and protein synthesis (17, 18). In general, ribosomal run-off and transit times are slower upon H_2O_2 exposure, but stress-regulatory factors are preferentially associated with ribosomes, suggesting increased translation. Several RNA-binding proteins play essential roles during oxidative stress (19), but their specific actions and targets are often unknown.

Cellular protein concentrations are also affected by proteolysis. The proteasome is the main protease complex responsible for degradation of unfolded, damaged and unneeded intracellular proteins in eukaryotic cells. Proteasomal degradation decreases under strong oxidative stress and increases under mild oxidative stress (20). Non-degradable oxidized proteins are prone to cross-linking and aggregation, and the aggregates may interact with the proteasome, decreasing its efficiency (9). Although proteasome function is well-defined during normal proteolysis, the exact expression and functional response of the proteasome to oxidative stress is still a matter of debate (21, 22).

While these examples illustrate that protein expression with respect to translation and protein degradation is heavily affected during oxidative stress, only a few small-scale measurements of protein concentration changes in response to oxidative stress exist to-date, and these studies do not compare protein levels to transcript levels (23-26). Time-dependent proteomics measurements with matching mRNA data are still scarce (27, 28). We provide the first time-resolved concentration measurement of >1,900 yeast proteins during two hours after diamide-induced oxidative stress. We focus on protein expression changes, as the transcriptional response has been described extensively elsewhere (14). Integrating our measurements with transcription (14, 29), translation (16, 30) and other regulatory data, we characterize the general and specific proteome response to oxidative stress, highlighting possible regulatory mechanisms and their targets. We characterize expression patterns of groups of proteins and individual examples, such as Tsa1, a multi-functional protein involved in oxidative stress resistance (31), genomic instability (32), apoptosis protection (33), and prion formation (34).

METHODS

Transcript concentrations from published microarray data

Transcript information was taken from a published dataset (14). The data is relative, i.e. measurements refer to expression levels at time = 0min. To estimate absolute mRNA concentrations, we multiplied the relative values at each data point with the expected average concentration of the mRNA under unperturbed conditions, as has been done previously (35). The data used in this study (14) correlates well with transcriptomics data from other studies (36, 37)(*not shown*) indicating that yeast mRNA expression changes measured in different laboratories are comparable.

Protein concentrations from quantitative shotgun proteomics experiments

Proteomics experiments were performed on yeast grown in conditions identical to those used by Gasch et al. (14). Briefly, we grew yeast DBY7286 cells to early log-phase in rich medium (YPD), treated them with 1.5 mM diamide and collected 100 ml cell culture at 0, 10, 20, 30, 40, 60, 90 and 120 min. Cells were still in logarithmic growth phase when harvested (*not shown*). From each fraction we extracted total soluble protein as described before (38). Cells were disrupted using glass beads, and cellular lysate was extracted by centrifugation at 5,000 g for 50 min. Lysis buffer consisted of 25 mM Tris-HCl pH 7.5, 5 mM DTT, 1.0 mM EDTA, 1X CPICPS (Calbiochem protease inhibitor cocktail, Sigma). Protein concentration was measured and lysate diluted to 2 mg/ml with buffer (50 mM Tris-HCl, pH 8.0). 50 μl of diluted cell lysate was mixed with 50 μl of 100% trifluoroethanol and incubated at 55 °C for 45 min (15 mM DTT). The sample was cooled to room temperature and incubated with 55 mM iodoacetamide in dark for 30 min. The sample was then diluted to 1 ml with buffer (50 mM Tris-HCl, pH 8.0) and 1:50 w/w Trypsin was added to digest for 4.5 hrs at 37 °C. Tryptic digestion was halted by adding 2% v/v formic acid. The sample was lyophilized to 20 μl, resuspended in buffer C (95% H_2O, 5% acetonitrile, 0.01% formic acid) and washed using a HyperSep C18 spintip (Thermo Fisher). The eluted sample was again lyophilized to 10 μl, resuspended in 120 μl buffer C and filtered through a Microcon-10 filter at 12,000 g. The sample was stored at -80 °C until LC-MS/MS analysis.

LC-MS/MS analysis. Samples were injected into an LTQ-Orbitrap Classic (Thermo Electron) mass spectrometer and analyzed in a 5 to 90% acetonitrile gradient over five hours via reverse phase chromatography on a Thermo BioBasic-18 column 150 mm x 0.10 mm ID. Each of the runs was analyzed independently with Bioworks (Thermo Fisher), searching a database of yeast protein sequences (SGD, 2009). The results were combined for analysis by PeptideProphet (39), ProteinProphet (40) and post-processed in the APEX pipeline (35, 41) to estimate absolute and differential protein expression based on spectral counts. We accepted proteins as confidently identified if the ProteinProphet probability was above a cutoff corresponding to <5% global false discovery rate. Absolute protein concentrations were normalized to an average of 4,000 molecules/cell based on published estimates (35, 42). Relative protein expression changes are calculated with respect to measurements at time = 0 min, log-transformed and normalized to mean 0 and standard deviation 1. Significance of expression changes was calculated (relative to the measurement at time = 0 min) according to the method by Lu et al. (35). Cysteine-containing peptides were extracted from the prot.xml files provided by the software.

We conducted the experiment twice (biological replicates), and collected several technical replicates (repeat mass spectrometry measurements). The raw data is published at http://www.marcottelab.org/MSdata/, as Dataset 15. The pepxml files are uploaded on Tranche (ProteomeCommons), data hash: Zz/J8b5YBb8yRqW4IukAw17Mzk56f/ItjicIy8v87h1aXAxgrj8Hcbin323ovJR4ZBcdl9yVMppGza9REHxiqhOJj7UAAAAAAAAW6w==. More information on experimental replicates is provided in the **Supplement (Notes section, Figure S1).** Basic mass spectrometry data is provided in **Supplementary Data File 2**.

Data processing and analysis

Earlier work has shown that protein concentrations are expected to be accurate within two-fold on average (35) which is the lower boundary of expression changes that we would consider biologically meaningful. For 69% of the proteins, concentrations vary less than two-fold across replicates (**Table S1**). High quality and reproducibility of the individual files from both biological and technical replicates allowed for pooling of all datasets to increase coverage (**Figure S1**). Pooling of datasets has the advantage that for a given protein whose identification is sub-threshold in individual datasets, the combined information from all datasets may be strong enough to push it above threshold. Details on data quality control are presented in the **Supplement (Figures S1-S5, Tables S1-S4)**.

Auto-correlation (**Figure 2**) was calculated using log-transformed absolute expression values, comparing protein and mRNA expression vectors of different time points against the vector at time = 0 min. We clustered the column-normalized expression profiles using ClusterX (43), extracting clusters with a correlation coefficient $|R| \geq 0.80$ (**Figure 1**). Prior to clustering, absolute expression data was smoothed and then back-transformed into relative, log-normalized expression values. Smoothing involved re-calculation of each data point as the average of the preceding and following data point, i.e. concentration (t) = average (concentration at t-1, t, t+1) (moving-average method). **Figure 1** shows smoothed log-normalized relative expression data; **Figure 3** shows raw (un-smoothed) data that has been log-normalized (base 10). The goal of our analysis is to reveal general trends in time-dependent mRNA and protein expression. For that reason, we chose the simple, but relatively drastic 'moving-average' smoothing method to eliminate noise in the data. The moving-average method enables us to extract strong trends that are consistent across many genes (e.g. the drop in protein concentration at 20 min in cluster C). The method has the disadvantage that it dampens subtle expression differences of individual genes within one cluster, e.g. those observed for Ccs1 and Sod2 (Figure 3B, C, respectively). For that reason we present the un-smoothed data in **Figure 3** to enable the reader to view the original data.

To create a random model, we shuffled gene identifiers for the proteomics data and repeated the clustering with the new, synthetic mRNA-protein profiles (**Figure S7**). Function analysis was performed with FuncAssociate (44). Reported function enrichments were significant with P-value<0.001.

We compiled a set of expression attributes (features) which we used to characterize cluster membership and to reveal possible underlying regulatory mechanisms. These attributes included both sequence based and experimental attributes (**Table 1**). We excluded features that were invariant across any of the 815 genes in the core dataset (e.g. targets of several chaperones and RNA-binding proteins), and features that showed high correlation to other features (R>0.90), e.g. FOP and Codon Bias Index.

To learn cluster membership, we used the WEKA machine learning software (45). Bagging with RandomForest performed best (**Figure S8**). When learning individual (binary) cluster-membership (member of cluster or not, {1,0}), we used cost-sensitive learning with a confusion matrix adjusted to number of positives in the training data. Ten-fold cross-validation was used to evaluate learning success. The F-measure of prediction is the harmonic mean of precision and recall, calculated as *F = 2*precision*recall / (precision+recall)*. The closer the F-measure is to 1, the better is the prediction. Similarly, the closer the Area Under the Curve (AUC) of a ROC plot is to 1, the better the prediction (**Table 2**).

Attribute (feature) selection was also conducted in cost-sensitive manner (CostSensiviteSubsetEval), using GreedyStepwise and CfsSubsetSelection as search and evaluator algorithm, respectively. Attribute selection cannot be evaluated for statistical significance, but the 'merit' of the selected subset of features indicates the relative success of the procedure. After testing learning with all 157 features, we selected a subset of 17 features with the strongest predictive ability. **Table 2** lists the t-test scores for these 17 features for the three main clusters. Note that these features do not necessarily represent all features with significant t-test scores (provided in **Supplementary data file 1**), but they are those that enable prediction of membership in the clusters. The **Supplement** also describes further details on clustering, learning algorithms, feature selection, etc (**Figure S8, Tables S5-7**).

Sequence motifs were identified using MEME (46) with the settings 'any number of repetitions' and $4 \leq$ width ≤ 10 (**Figure S12**). **Supplementary data file 1** contains detailed information on the dataset of this study. The **Supplementary data file 2** contains primary information on peptide and protein assignments.

RESULTS AND DISCUSSION

Concordance and discordance between protein and mRNA expression changes

Our experiments produced absolute protein expression data for a total of 1,907 proteins. **Figure 1** shows the normalized, log-transformed expression changes for both mRNA (14) and protein expression for a core set of 815 proteins that have data available for ≥6 of the eight time points. Protein concentrations cover five orders of magnitude (**Figure S4**) and show a maximum of ~200-fold expression change. Even after accounting for delays due to translation, most proteins (>80%) have protein expression profiles that are very different from their corresponding mRNA expression profiles (**Figure 1, Figures S6, S7**), suggesting extensive regulation at the level of translation and protein degradation.

Transcript and protein expression responses display very different kinetics, as evidenced by an auto-correlation analysis (**Figure 2**). Most transcriptional changes occur at ~30 min after stress induction, indicated by the lowest auto-correlation at this time point (**Figure 2**). Ninety minutes after treatment, many transcript abundances have returned to normal levels (high auto-correlation) – consistent with previous results on transcription and mRNA degradation (29). In contrast, most of the protein expression response is much slower (**Figure 2**), and expression profiles continuously diverge even two hours after treatment. For many proteins, we observe strong protein abundance changes at 10 to 20 min after treatment (see examples below) which is later complemented by different expression patterns. This first and early response occurs entirely at the protein level, before the majority of the transcription response. For individual proteins, we observe a 10 to 20 min delay between the mRNA and protein response (**Figure S7**). In contrast to transcript abundances, concentrations for many proteins are not yet back to normal even two hours post-stress treatment. Since we did not continue our measurements beyond two hours, we cannot directly compare the expression changes to those from a previous study using rapamycin (28).

Despite conducting the experiment in log-phase, some of the observed expression changes may not be due to an oxidative stress response, but to changing conditions in the batch culture. Although recent work has shown that exponential growth in batch culture is a good model of steady-state (47), future studies may conduct the experiments in continuous growth culture or include further controls at additional time points. We also note that our method estimates concentrations of unmodified proteins – proteins that are heavily post-translationally modified will not be detected and lower the apparent concentration. (However, see discussion on cysteine oxidation below).

Similar to transcript abundances (14), protein abundance profiles show distinct clusters of co-regulated proteins (**Figure 1**). We observe 12 clusters with ≥10 members whose combined mRNA and protein expression profile are highly similar ($R \geq 0.80$, smoothed data) (**Figure S10**). The three largest clusters, called A, B, and C, have 127, 76, and 66 members respectively, and are described in detail below. Proteins in these clusters have distinct characteristics (**Table 2**), including functional biases (P-value < 0.001). **Figure 3** shows for each cluster examples of proteins with roles during the oxidative stress response. The clusters describe approximate expression patterns; the expression for individual proteins within each clusters may vary. In contrast to the smaller clusters, membership in clusters A, B, C can be predicted using a subset of 17 of the 157 expression attributes that we compiled (**Table 1, 2**). The tested features include amino acid composition, codon bias, targets of RNA-binding proteins or chaperones, RNA-secondary structure, measures of transcript and protein stability as well as translation efficiency. Features with predictive power suggest molecular mechanisms that may cause the observed expression patterns.

Genes with decreasing protein and mRNA abundance

Cluster A

The largest cluster (A, 127 proteins, **Figure 3A**) is strongly enriched for ribosomal proteins, translation factors, and tRNA synthetases (P-value < 0.001, **Table S5**). Both protein and mRNA abundances are immediately down-regulated after stress treatment; mRNA abundances start returning to normal at ~40 min. Cluster membership can be predicted well (AUC = 0.80, **Table 2**). Ribosomal proteins are generally highly abundant under normal conditions, in accordance with their genomic sequences that are characterized by high codon adaptation indices, little structured 5'UTRs, and high protein production rates (**Table 2**, P-value < 0.001, |t-value|>3.40). However, proteins in cluster A are also significantly less stable than proteins from clusters B and C, as indicated by their high intrinsic structural disorder (48) (P-value < 0.001, |t-value|>3.40). Such instability is consistent with the observed decrease in protein abundance, despite recovery of the mRNA levels. In response to mild oxidative stress, translation efficiency decreases in cluster A, as measured through ribosomal association with the mRNA (30). Decreasing translation and short protein half-lives explain the decrease in protein abundance despite recovery of mRNA expression levels (**Table 2, Figure 3A**).

Figure 3A shows examples of cluster A: two amino acyl t-RNA synthetases (Gln4, Ils1), two ribosomal subunits (Rps11b, Rps2) and the eukaryotic translation initiation factor 4B (Tif2). In mammals, eIF4B is a target of the RNA-binding protein TIAR, down-regulating translation (19, 49). In yeast, Tif2 mRNA is also a target of Lhp1 as discussed below.

Members of cluster A are targets of significantly more RNA-binding proteins than the average protein in the dataset (P-value < 0.001, **Supplementary data file 1**). One significant predictor of cluster membership is the RNA-binding protein Lhp1. Lhp1, the La homologous protein, is required for maturation of tRNA and U6 snRNA precursors, and it acts as a molecular chaperone for RNAs transcribed by polymerase III (50, 51). Lhp1 is required for the normal pathway of tRNA maturation through protection of nascent transcripts from exonucleolytic degradation. Lhp1 also binds the coding RNAs of a number of genes and gene families, including ribosomal mRNAs, Hac1 and other genes involved in the unfolded protein response, and its own Lhp1 transcript (52). Lhp1 targets are significantly enriched in cluster A (54/126, P-value < 0.001), explaining Lhp1's predictive power for cluster membership. One can hypothesize that Lhp1 may stabilize coding mRNAs in a manner similar to its chaperone function with non-codingh RNAs, resulting in the observed increase in mRNA levels after 40 min (**Figure 3A**).

Furthermore, targets of the RNA-binding protein Khd1 are significantly depleted in cluster A (P-value<0.001, |t-value|>3.40) making it a predictor of cluster membership (**Table 2**). Khd1 has been shown to repress translation of bud-localized mRNAs (53, 54) which is consistent with the presence of many highly abundant proteins (i.e. ribosomes) in cluster A.

Secondary structures in both the coding and untranslated regions impact transcript stability and translation efficiency. Indeed, a significant lack of secondary structures in the 5'UTR may support high translation initiation amongst cluster A proteins (**Table 2**, P-value < 0.001, |t-value|>3.40). Cluster A also has some members with a large number of secondary structures, i.e. RNA double-strands, in the coding strand (**Table 2**, P-value < 0.001, |t-value|>3.40) – the biological reason behind which remains to be investigated.

Finally, proteins in cluster A are significantly enriched in arginine (P-value < 0.001, |t-value|>3.40) and, accordingly, have a higher isoelectric point than other proteins (**Table 2**). Ribosomal proteins and translation factors, which are abundant in cluster A, bind to RNA, and many RNA-binding domains in these proteins are rich in arginine, e.g. in the RG, RGG or RS motifs (55).

Genes with decreasing mRNA and constant or increasing protein abundance

Features common to clusters B and C

Clusters B and C have several characteristics in common that distinguish them from cluster A (**Table 2**, **Figure 3BC**). They both are significantly enriched in proteins of the direct stress response (P-value<0.001, **Table S5**): cluster B contains many oxidoreductases and chaperones, while cluster C contains many proteases. Both clusters feature short-term up-regulation of mRNA abundance during the first 20 to 40 min, followed by transcript degradation (**Figure 3BC**). However, the protein expression profiles for these two clusters are very different.

Clusters B and C are each only about half to two-thirds the size of cluster A, and their membership is less easily predicted (**Table 2**). Proteins in both clusters have a low degree of intrinsic disorder, suggesting high protein stability (**Table 2**). The mRNAs in both clusters are also significantly more stable than other mRNAs under normal conditions (**Table 2**, P-value < 0.001, |t-value|>3.40), in contrast to the transcript response to stress (**Figure 3BC**). Thus transcript stability may be subject to stress-related regulation.

Clusters B and C are also enriched for binding sites of the poly(A)-binding protein Pab1 (**Table 2**), and all three clusters show binding sites for another poly(A)-binding protein Pub1. We could not match any other motifs to putative regulators (**Figure S12**). Pab1 binds to the poly(A) tails of mRNAs and interacts with eIF4-G to promote (cap-dependent) translation initiation (56) – consistent with the stable or increasing protein levels in clusters B and C compared to the decreasing protein levels in cluster A. Pab1 also affects formation of stress granules (57) and it has been implicated in cap-independent translation through binding to an A rich element in the 5'UTR (58) – which we observe in cluster B (**Table 2**). Pab1's own expression is only slightly affected by oxidative stress, and it is not member of clusters A, B, or C (*not shown*).

Cluster B

To cope with stress induced by thiol oxidation, a diverse set of antioxidant responses is triggered in yeast. Several antioxidant genes (peroxidases, disulfide reductases, chaperones) are up-regulated and grouped together in cluster B. In cluster B, protein levels increase during the first 30 min, although many proteins have a 20 min lag in their response (**Figure 3B**). At later time points, protein levels are constant or slightly decreasing. Cluster B contains one of the primary enzymes in the oxidative stress response, superoxide dismutase Sod1, and its chaperone, Ccs1 (**Figure 3B**). Both proteins are essential for developing resistance against oxidative stress (59).

Ccs1 is necessary for the folding of Sod1, forming active Sod1 from an apo-protein (60). Protein expression is consistent with this function, Ccs1 is present when Sod1 is present (**Figure 3B**).

Besides Ccs1, two yeast glutaredoxins, Grx1 and Grx2, influence Sod1 function (61). These enzymes catalyze the reduction of intra- and inter-protein disulfides and low-molecular-weight thiols such as glutathione which is produced in abundance during diamide-induced stress (62, 63). Grx1 and Grx2 can, similar to NADPH and thioredoxins, stimulate translation (64), and Grx2 may be regulated through in-frame start codons (65). While the two enzymes have highly similar sequences (66), they differ in their structure and biochemical activity (67), and Grx2 accounts for most of the glutathione-dependent oxidoreductase activity (68). The functional difference is also reflected in the expression data, where Grx2 has a stronger response than Grx1 both at the mRNA and protein level (**Figure 3B**). Both enzymes show stabilized protein expression levels compared to decreasing transcription 40 min after treatment, suggesting that protein stability is regulated. We find, for example, that Grx2 has fewer PEST degradation sites than the average protein (**Supplementary data file 1**).

In addition to glutaredoxins, mRNAs are up-regulated for thioredoxins and glutathione oxidoreductases who fulfill crucial antioxidant roles during diamide-induced stress. In contrast to mRNA levels which decrease slowly 30 min after treatment, protein concentrations remain constant, suggesting high protein stability or an increase in translation rate per available mRNA. Our dataset comprises some members of the thioredoxin and glutathione systems: two peroxidases (Ahp1 and Gpx3) and thioredoxin 2 (Trx2), a cytosolic disulfide reductase; thioredoxin reductase 2 (Trr2) and glutathione reductase (Glr1), enzymes that catalyze the final step in both systems' reduction cascade (69); and also the glutathione synthetase (Gsh2).

Figure 3B shows Zwf1, the glucose-6-phosphate dehydrogenase that catalyzes the first, irreversible and rate-limiting step of the pentose phosphate pathway (70) which is an essential component of oxidative stress resistance (71, 72). Zwf1 is involved in maintenance of cytosolic levels of NADPH which in turn is electron donor to several anti-oxidant systems. Despite decreases in mRNA abundance for 30 min after stress treatment, Zwf1's protein levels remain stable throughout the entire measurement time (**Figure 3B**). Zwf1's stability may possibly be linked to it being bound by eleven chaperones – more than observed on average for the proteins in our dataset (average is four chaperones per protein, **Supplementary data file 1**).

Cluster B shows some enrichment in secondary structures in the 5'UTRs of its member mRNAs, as well as depletion of structures in the first ten nucleotides of the coding region. Secondary structures in the 5'UTR are thought to hinder translation (73), thus the increase in protein levels may derive from protein stability regulation and not translation increase.

Cluster C

Cluster C is enriched for components of the proteasome (**Table 2**). The 26S proteasome holoenzyme is a multisubunit protease composed of the 20S catalytic core capped with the 19S regulatory particle which recognizes ubiquitin-tagged proteins. While the exact role of the proteasome during oxidative stress is still a matter of debate, most authors suggest that only the 20S proteasome is responsible for the hydrolysis of oxidized proteins in an ubiquitin- and ATP-independent fashion (74, 75). The 26S proteasome, i.e. capped with regulatory particles, is more stress sensitive than the 20S core (76, 77), and we observe no or only few copies of 19S subunits in our data (*not shown*).

Protein expression of subunits of the 20S core in cluster C (**Figure 3C**) sharply decreases during the first 20 min, but recovers at 30 min and is constant for the rest of the measurement time. The stabilized protein levels seem necessary to cope with the increasing levels of oxidatively damaged proteins. The 'dip' in proteasome abundance at 20 min is only present at the protein level, and not at the mRNA level – and it is a marked characteristic of cluster C (**Figure 3C**). It is most pronounced amongst subunits of the 20S proteasome, but also visible amongst other members of cluster C, e.g. transport proteins or superoxide dismutase 2.

We cannot tell from the data if the proteasomal subunits are truly degraded, change localization, or are modified (e.g. through cysteine oxidation) and subsequently escape mass spectrometric detection. The observed changes in protein concentrations are not accompanied by changes in the fraction of cysteine-containing peptides (**Figure S5**), thus cysteine-oxidation does not influence the measurements of protein concentrations. The 20S proteasome is, however, sensitive to oxidative stress, and its S-glutathiolation can affect proteasome activity (78, 79). Oxidation of cysteines by diamide can impair protein function (2) and may trigger degradation of proteins. Little is known to-date about degradation of the proteasome and its regulation, i.e. if it occurs primarily by the lysosome (80) or by the proteasome itself (81). The increase in protein concentrations at later time points (**Figure 3C**) may occur through replenishment via translation, reversal of the amino acid modifications, or protein localization changes.

The characteristic dip in protein expression also occurs in non-proteasomal stress proteins, for example the peroxiredoxins Ahp1 and Tsa1 (**Figure 3C**). Tsa1 is a key regulator of the oxidative stress response, and an understanding of its regulation is of great importance. Tsa1 is generally expressed at high levels (82). Our data shows a discrepancy in Tsa1's protein and mRNA expression regulation. Protein abundance decreases at first, but then consistently increases throughout the measurement, contrasting the transcription down-regulation one hour after treatment. The Tsa1 mRNA can be bound by five different RNA-binding proteins, amongst which Yra1 and Mex67 may be regulators of post-transcriptional changes in concentration of the protein (83, 84)(**Supplementary data file 1**).

CONCLUSIONS

Our work provides a large-scale, time-resolved dataset of yeast protein expression in response to oxidative stress. The protein measurements map directly to a transcriptome study which employed identical conditions (14), describing eight time points over two hours after diamide treatment. Due to the intrinsic bias of mass spectrometry towards high-abundance proteins, many transcription factors (of low abundance) are not included, but their roles in the oxidative stress response have been described elsewhere. Our analyses focus on protein expression changes beyond what can be explained by transcript changes, i.e. we examine the results of translation and protein degradation.

Overall protein expression changes reflect what is expected from the oxidative stress response: down-regulation of translation (cluster A), up-regulation of oxidoreductases, chaperones (cluster B), the proteasome, and other stress-response proteins (cluster C) (**Figure 1, 3**). However, for at least one third of the genes in the dataset, the time-dependent mRNA and protein expression profiles are different from each other (**Figure 1, Figure S7**) and mRNA and protein fold-changes differ by up to two orders of magnitude (*not shown*), suggesting extensive regulation at the level of translation and protein degradation. Typical stress experiments monitor transcript changes 30 to 60 min post treatment. Protein concentrations in our data often continue to change until two hours post treatment (**Figure 2**) – an observation to be considered when designing stress experiments.

Integrating the mRNA and protein expression profiles with features of translation and protein degradation (**Table 1**), we predicted membership in regulatory clusters for 41% of the proteins in the core dataset (270/651) with 0.66 to 0.88 AUC, i.e. the probability that the classifier will rank a random positive instance higher than a random negative instance (**Table 2**). Predictive features focused on translation and protein degradation, as we did not aim to explain changes in transcription. However, many of the features likely play a role both in transcript and protein expression regulation.

The 17 most predictive features included protein stability (measured as the presence of unstructured loops), RNA secondary structures in the 5', 3' UTR and the coding sequence (measured as double-strandedness), general mRNA half-life and translation efficiency under unperturbed conditions, and binding of the RNA-binding proteins Lhp1 and Khd1 (**Table 2**). Changes in translation efficiency in response to menadione (30), but not hydrogen peroxide (16), were predictive of cluster membership, suggesting similarity between the diamide and menadione response. Interestingly, the predictive features did not include the 50 chaperones for which target data is available (85), suggesting that they have only a minor role in targeted protein expression regulation. This observation may change with future, more complete chaperone datasets.

While much previous work has demonstrated general down-regulation of translation and translation regulators, e.g. phosphorylation of translation initiation factors (86), there is much less information on the specific effects of translational regulation during stress. Our dataset resolves some of the discrepancies between mRNA expression and protein activity, and we provide hints for some regulatory mechanisms. The proteomics measurements are sensitive enough to describe the detailed dynamics of protein concentration changes that have been missed by transcriptome analysis, for example the temporary decrease in concentrations of reactive cysteine-containing proteins such subunits of the 20S proteasome.

For individual proteins, e.g. Tsa1, the proteomics data corroborate classic biochemistry experiments (87, 88) and provide additional information on the time-dependent protein expression changes. The transcript and protein expression profiles for Tsa1 differ substantially (**Figure 3C**) which could be caused by changes in protein localization, stability, translation, and by post-translational modifications. Future studies may provide many more time-resolved proteome measurements which will help our understanding of general and specific post-transcriptional expression dynamics. They will also help understanding even more intricate processes such as the long-term adaptation of cells to stress, involving translation (89) and protein degradation regulation.

ACKNOWLEDGEMENTS

We thank Audrey Gasch for kindly providing the yeast strain. We thank John Prince, Daniel R. Boutz, and Rebecca Bish for help and advice. CV acknowledges funding by the International Human Frontier Science Program.

FIGURES / TABLES

Note: higher-resolution figures are attached at the end of the document

Figure 1. RNA and protein expression show distinct patterns

The matrix shows the normalized logarithmic expression changes for both mRNA (left, (14)) and protein (right, this study) relative to time=0min. Each row denotes one gene, each column one time point (in min). The total number of genes is N=815; non-smoothed data is shown in **Figure S3**. The red rectangles indicate the approximate position of the three largest clusters with vector similarity of R>0.80. These clusters are characterized in **Table 2**. Grey denotes missing values.

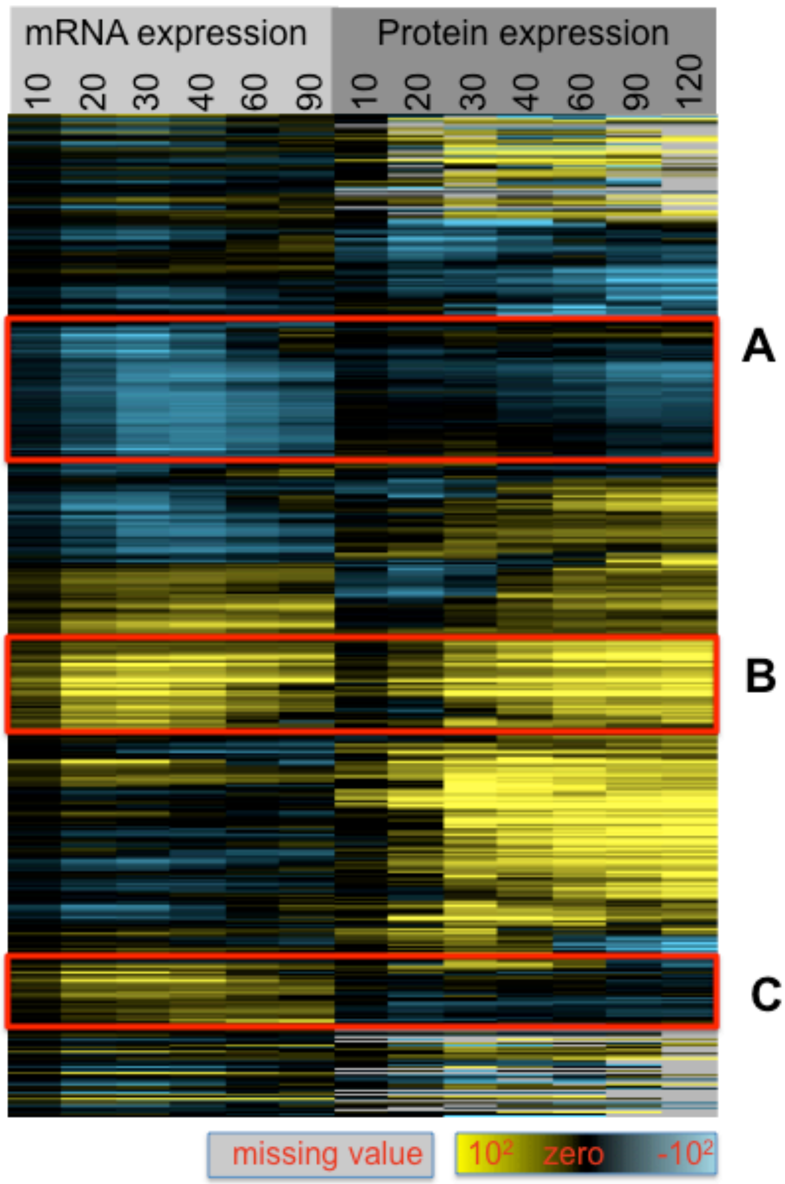

Figure 2. Different dynamics of the transcriptome and proteome response

For both the protein and the mRNA expression profiles, we calculated Pearson's correlation coefficients (R^2) to describe similarity between expression vectors ($\log_{10}$ of absolute values) at different time points compared to the vector at time=0min. **Figure S5** shows auto-correlation for other transformations of the data.

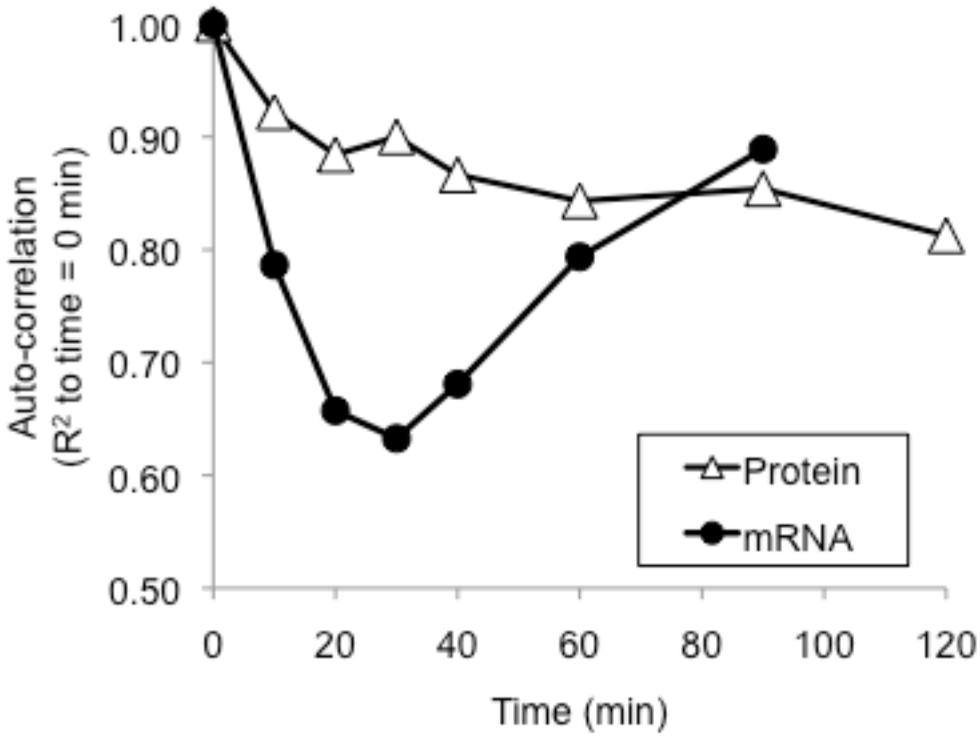

Figure 3. Examples of proteins from the three largest clusters

For each cluster we selected example proteins whose expression changes are interesting within the context of the oxidative stress response. The graphs show the normalized logarithmic change (log base 10, time point vs. time point 0) of mRNA (left) and protein (right) expression. Properties of the three main expression clusters are described in **Table 2**. Scales are adjusted to be the same across each row. The mRNA expression pattern of Ccs1 deviates from the average expression in cluster B which may be an artifact of hierarchical clustering.

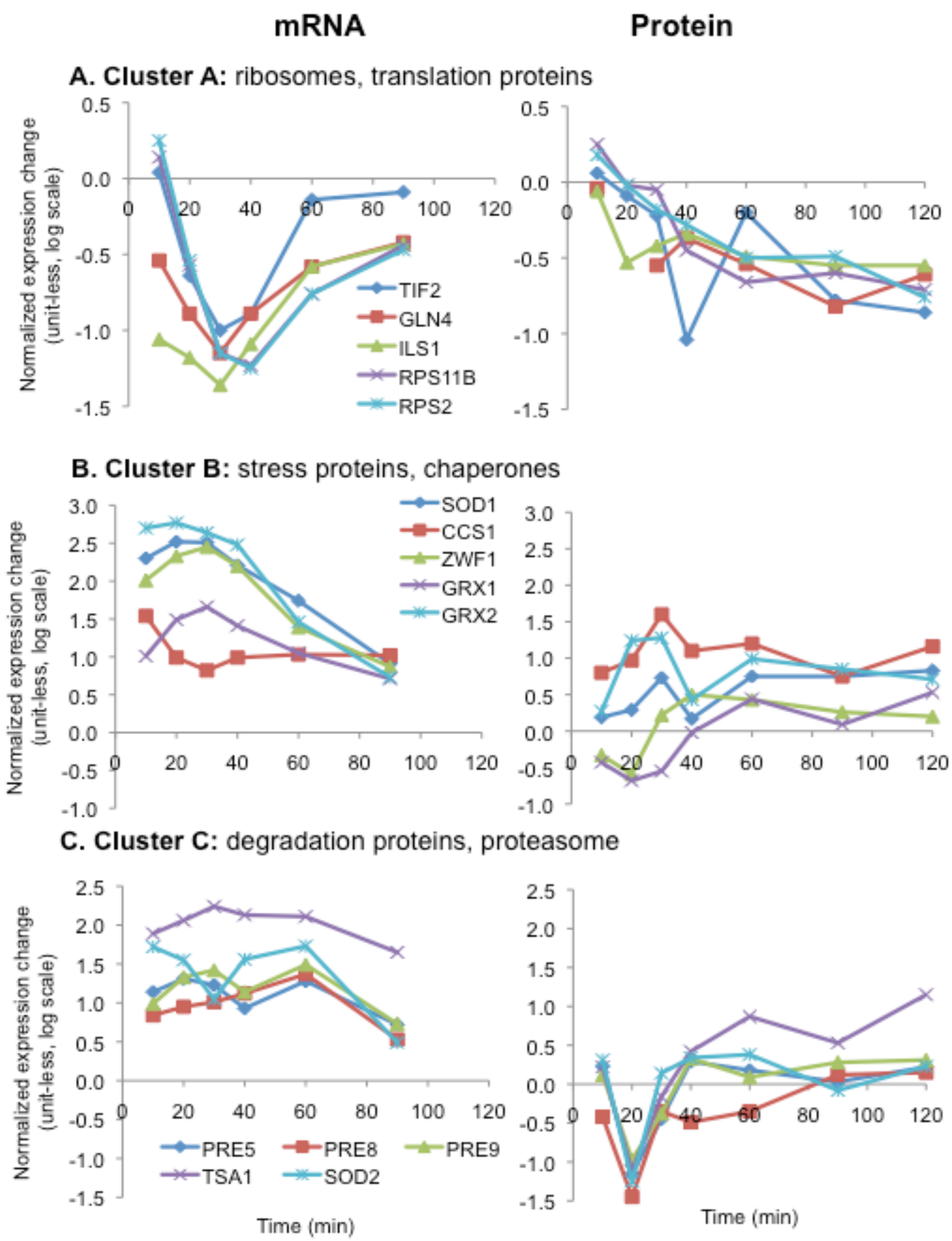

Table 1. Potential predictors of translation and protein degradation regulation

A total of 157 attributes were analyzed in their ability to explain membership of proteins in expression clusters as identified in the data in **Figure 1**. We assembled experimental datasets as well as sequence features that are known to relate to post-transcriptional expression and protein degradation. These attributes include binding of RNA-binding proteins (putative regulators), protein stability estimates (experimental and theoretical), measurements of translation efficiency and transcript stability, sequence features, and few other features outside these categories. References are provided in brackets. DISEMBL – DISorder predictor from the European Molecular Biology Laboratory; MIPS – Munich Institute for Protein Sciences; uORF – upstream Open Reading Frame; PARS – Parallel Analysis of RNA Structure (experimental measure of double-strandedness in RNA); PEST – Proline, Glutamate, Serine, Threonine degradation signal; RBP – RNA binding protein; UTR – Un-Translated Region

Data type	Source / Comment
Target of RNA-binding protein	Possible regulators of transcript stability and/or translation efficiency
Rab1	MIPS (90)
Bfr1, Cbc2, Gbp2, Khd1, Nab2, Nab3, Npl3, Nrd1, Nsr1, Pab1, Pub1, Puf4, Scp160, Sik1, Yra2	Targets chosen at <1%FDR (54) (54)
Lhp1	(52)
Yra1, Mex67	(91)
Khd1	(53)
Total number of RBP regulators	across above studies
Protein stability	
Protein half-life	Measure of protein stability (92)
PEST protein degradation signal	Maximum score in ePESTfind (93)
DISEMBL coils, DISEMBL hot-loops	Disordered proteins tend to be less stable than folded proteins, and vice versa. Disorder is measured by loops/coils and "hot loops" (loops with a high degree of mobility) as predicted by DisEMBL (94).
Chaperones: APJ1, CAJ1, CCT2, CCT3, CCT4, CCT5, CCT6, CCT7, CCT8, CWC23, DJP1, ECM10, ERJ5, GIM3, GIM4, GIM5, HLJ1, HSC82, HSP104, HSP12, HSP26, HSP31, HSP42, HSP60, HSP78, HSP82, JAC1, JEM1, JID1, JJJ1, JJJ2, JJJ3, KAR2, LHS1, MCX1, MDJ1, PAC10, PFD1, SCJ1, SEC63, SIS1, SNO4, SSA1, SSA2, SSA3, SSA4, SSB1, SSB2, SSC1, SSE1, SSE2, SSQ1, SSZ1, SWA2, TCP1, TIM14, XDJ1, YDJ1, YKE2, ZUO1; Number of chaperones bound to protein	Targets of chaperones may be stabilized (85)
Translation and transcript stability	
Translation efficiency change (measured as ribosome profile: $\log_{10}$[PS+MS/PC+MC])	Translational response to 0.2mM H_2O_2 stress (16) (>2-fold change)
Translation efficiency change (ribosome association as $\log_2$[stress/control])	Translational response to menadione stress (30)
Protein production rate (proteins/sec); Numbers of proteins per mRNA per section (protein production/transcription rate), $\log_{10}$[protein/mRNA]	General translation efficiency (95-97) (unperturbed system)
mRNA half-life (poly-A length measurement)	General transcript stability (98) (unperturbed system)
Number of uORFs; Conserved uORFs	Influencing translation efficiency (99)
Sequence lengths (UTRs, coding)	Influencing protein expression: the shorter the sequence, the more protein (38)
Number of motifs in 3'UTR	Possible regulators of transcript stability or translation efficiency (100)
Minimum free energy (50 nucleotides at end of 5'UTR, beginning of coding strand, and at beginning of 3'UTR)	RNA secondary structure influences transcript stability and/or accessibility to regulators and ribosomes (73)
PI, CAI, relative amino acid frequencies, FOP score, GRAVY score, AROMATICITY score	*Saccharomyces* Genome Database (101)
Other features	
Essentiality	Gene knockout effect under normal conditions (102)
Growth score during diamide treatment, Sensitivity to diamide treatment, Effect unique to diamide treatment Indicating role of gene in diamide resistance (growth)	(71)
PARS score in the coding region, 3' and 5'UTR. Calculated were average, standard deviation, relative standard deviation, minimum, maximum, median score across the whole sequence, the first and last ten nucleotides of the sequence.	The higher PARS score, the higher the probability of nucleotides in the sequence to be in double-stranded conformation. RNA secondary structure influences transcript stability and/or accessibility to regulators and ribosomes (103)

Table 2. Characteristics of the three largest clusters

The three largest clusters of expression patterns (R>0.80) as indicated in **Figure 1** (out of 12 clusters with >10 members). Function enrichment analyzed with FuncAssociate (P-value<0.001) (44). The F-measure is the harmonic mean of precision and recall. Combined prediction aims to predict membership for all 12 clusters simultaneously, i.e. membership in cluster {A, B, C, D, ...}; individual predictions predict membership of a gene in one cluster at a time, i.e. in cluster A {yes, no}. All attributes (features) used are listed in **Table 1** with more detailed descriptions. The value listed next to the selected attribute describes the result of a t-test. A t-value > |3.40| is significant at the P-value<0.001 level for all three clusters (given the cluster size) and is printed in **bold**. Negative and positive t-values indicate depletion and enrichment of the feature in the test set, respectively. $[T]_{5-10}$ and $[TA]_{3-6}$ are binding motifs for the poly(A)-binding proteins Pub1 and Pab1, respectively (54). AUC – Area Under Curve (where curve is the Receiver-Operator Characteristic), the closer to 1 the better is the prediction; PARS – Parallel Analysis of RNA Structure, i.e. experimental measure of double-strandedness in RNA taken from reference (103)

	Cluster A	Cluster B	Cluster C
Cluster size	127	76	66
Combined prediction (157 features)			
F-Measure	0.65	0.14	0.08
AUC	**0.85**	**0.65**	**0.78**
Individual prediction (17 features)			
F-Measure	0.66	0.33	0.06
AUC	**0.88**	**0.71**	**0.66**
Protein function enrichment	ribosome, translation	oxidoreductase, protein folding	proteases
<u>Attribute selection</u>			
Merit of best subset of attributes in prediction	**0.38**	**0.22**	**0.24**
<u>Subset of predictive features</u>			
Arginine content	**6.35**	**-6.19**	**-5.51**
Aspartate content	**-5.29**	1.53	-0.15
Codon Adaptation Index (101)	**14.05**	-2.11	0.06
DISEMBL hot loops (disorder measure) (94)	**6.24**	**-4.99**	**-2.95**
Target of Khd1 (53)	**-9.09**	-0.73	-0.28
Target of Lhp1 (52)	**6.14**	-0.97	-0.82
Logarithm of mRNA half-life under normal conditions (98)	**-5.79**	**5.47**	**3.57**
Logarithm of protein production rate under normal conditions (97)	**13.32**	0.59	**4.62**
PARS – average score in 5'UTR (103)	**-4.82**	3.27	0.89
PARS – average score amongst first 10 nt in coding sequence (103)	2.28	-2.68	1.86
PARS CDS – maximum score in coding sequence (103)	**18.00**	-0.68	2.44
PARS CDS – spread (standard deviation) of scores in coding sequence (103)	**13.18**	-1.77	2.98
PARS – spread (relative standard deviation) of scores in 3'UTR (103)	-1.20	-0.58	-0.54
Isoelectric point (101)	**6.51**	**-5.61**	**-5.43**
Translation efficiency under menadione stress (30)	**-4.58**	2.05	0.92
<u>Motif presence</u>			
In 5'UTR	$[T]_{5\text{-}10}$	$[T]_{5\text{-}10}$, $[TA]_{3\text{-}6}$	$[T]_{5\text{-}10}$
In 3'UTR	$[T]_{5\text{-}10}$	$[T]_{5\text{-}10}$, $[TA]_{3\text{-}6}$	$[T]_{5\text{-}10}$, $[TA]_{3\text{-}6}$

REFERENCES

1. Halliwell, B., and Gutteridge, J. M. C. (2007) *Free Radicals in Biology and Medicine*, Oxford University Press, New York, USA.
2. Sohal, R. S. (2002) Role of oxidative stress and protein oxidation in the aging process. *Free Radic Biol Med* 33, Page.
3. Costa, V., Quintanilha, A., and Moradas-Ferreira, P. (2007) Protein oxidation, repair mechanisms and proteolysis in Saccharomyces cerevisiae. *IUBMB Life* 59, Page.
4. Oyadomari, S., Araki, E., and Mori, M. (2002) Endoplasmic reticulum stress-mediated apoptosis in pancreatic beta-cells. *Apoptosis* 7, Page.
5. Terro, F., Czech, C., Esclaire, F., Elyaman, W., Yardin, C., Baclet, M. C., Touchet, N., Tremp, G., Pradier, L., and Hugon, J. (2002) Neurons overexpressing mutant presenilin-1 are more sensitive to apoptosis induced by endoplasmic reticulum-Golgi stress. *J Neurosci Res* 69, Page.
6. Li, H., and Guo, M. (2009) Protein degradation in Parkinson disease revisited: it's complex. *J Clin Invest* 119, Page.
7. Pockley, A. G. (2002) Heat shock proteins, inflammation, and cardiovascular disease. *Circulation* 105, Page.
8. van Tijn, P., Hol, E. M., van Leeuwen, F. W., and Fischer, D. F. (2008) The neuronal ubiquitin-proteasome system: murine models and their neurological phenotype. *Prog Neurobiol* 85, Page.
9. Grune, T., Jung, T., Merker, K., and Davies, K. J. (2004) Decreased proteolysis caused by protein aggregates, inclusion bodies, plaques, lipofuscin, ceroid, and 'aggresomes' during oxidative stress, aging, and disease. *Int J Biochem Cell Biol* 36, Page.
10. Stadtman, E. R. (2006) Protein oxidation and aging. *Free Radic Res* 40, Page.
11. Visconti, R., and Grieco, D. (2009) New insights on oxidative stress in cancer. *Curr Opin Drug Discov Devel* 12, Page.
12. Franssens, V., Boelen, E., Anandhakumar, J., Vanhelmont, T., Buttner, S., and Winderickx, J. (2010) Yeast unfolds the road map toward alpha-synuclein-induced cell death. *Cell Death Differ* 17, Page.
13. Barros, M. H., da Cunha, F. M., Oliveira, G. A., Tahara, E. B., and Kowaltowski, A. J. (2010) Yeast as a model to study mitochondrial mechanisms in ageing. *Mech Ageing Dev* 131, Page.
14. Gasch, A. P., Spellman, P. T., Kao, C. M., Carmel-Harel, O., Eisen, M. B., Storz, G., Botstein, D., and Brown, P. O. (2000) Genomic expression programs in the response of yeast cells to environmental changes. *Mol Biol Cell* 11, Page.
15. Smirnova, J. B., Selley, J. N., Sanchez-Cabo, F., Carroll, K., Eddy, A. A., McCarthy, J. E., Hubbard, S. J., Pavitt, G. D., Grant, C. M., and Ashe, M. P. (2005) Global gene expression profiling reveals widespread yet distinctive translational responses to different eukaryotic translation initiation factor 2B-targeting stress pathways. *Mol Cell Biol* 25, Page.
16. Shenton, D., Smirnova, J. B., Selley, J. N., Carroll, K., Hubbard, S. J., Pavitt, G. D., Ashe, M. P., and Grant, C. M. (2006) Global translational responses to oxidative stress impact upon multiple levels of protein synthesis. *J Biol Chem* 281, Page.
17. Nika, J., Yang, W., Pavitt, G. D., Hinnebusch, A. G., and Hannig, E. M. (2000) Purification and kinetic analysis of eIF2B from Saccharomyces cerevisiae. *J Biol Chem* 275, Page.
18. Lee, J. H., Pestova, T. V., Shin, B. S., Cao, C., Choi, S. K., and Dever, T. E. (2002) Initiation factor eIF5B catalyzes second GTP-dependent step in eukaryotic translation initiation. *Proc Natl Acad Sci U S A* 99, Page.
19. Abdelmohsen, K., Kuwano, Y., Kim, H. H., and Gorospe, M. (2008) Posttranscriptional gene regulation by RNA-binding proteins during oxidative stress: implications for cellular senescence. *Biol Chem* 389, Page.
20. Breusing, N., and Grune, T. (2008) Regulation of proteasome-mediated protein degradation during oxidative stress and aging. *Biol Chem* 389, Page.
21. Hosler, M. R., Wang-Su, S. T., and Wagner, B. J. (2003) Targeted disruption of specific steps of the ubiquitin-proteasome pathway by oxidation in lens epithelial cells. *Int J Biochem Cell Biol* 35, Page.
22. Ding, Q., Reinacker, K., Dimayuga, E., Nukala, V., Drake, J., Butterfield, D. A., Dunn, J. C., Martin, S., Bruce-Keller, A. J., and Keller, J. N. (2003) Role of the proteasome in protein oxidation and neural viability following low-level oxidative stress. *FEBS Lett* 546, Page.
23. Weeks, M. E., Sinclair, J., Butt, A., Chung, Y. L., Worthington, J. L., Wilkinson, C. R., Griffiths, J., Jones, N., Waterfield, M. D., and Timms, J. F. (2006) A parallel proteomic and metabolomic analysis of the

hydrogen peroxide- and Sty1p-dependent stress response in Schizosaccharomyces pombe. *Proteomics* 6, Page.
24. Mirzaei, H., and Regnier, F. (2006) Protein-RNA cross-linking in the ribosomes of yeast under oxidative stress. *J Proteome Res* 5, Page.
25. Kusch, H., Engelmann, S., Albrecht, D., Morschhauser, J., and Hecker, M. (2007) Proteomic analysis of the oxidative stress response in Candida albicans. *Proteomics* 7, Page.
26. Garcia-Leiro, A., Cerdan, M. E., and Gonzalez-Siso, M. I. (2010) Proteomic analysis of the oxidative stress response in Kluyveromyces lactis and effect of glutathione reductase depletion. *J Proteome Res* 9, Page.
27. Flory, M. R., Lee, H., Bonneau, R., Mallick, P., Serikawa, K., Morris, D. R., and Aebersold, R. (2006) Quantitative proteomic analysis of the budding yeast cell cycle using acid-cleavable isotope-coded affinity tag reagents. *Proteomics* 6, Page.
28. Fournier, M. L., Paulson, A., Pavelka, N., Mosley, A. L., Gaudenz, K., Bradford, W. D., Glynn, E., Li, H., Sardiu, M. E., Fleharty, B., Seidel, C., Florens, L., and Washburn, M. P. (2009) Delayed correlation of mRNA and protein expression in rapamycin-treated cells and a role for Ggc1 in cellular sensitivity to rapamycin. *Mol Cell Proteomics* 9, Page.
29. Shalem, O., Dahan, O., Levo, M., Martinez, M. R., Furman, I., Segal, E., and Pilpel, Y. (2008) Transient transcriptional responses to stress are generated by opposing effects of mRNA production and degradation. *Mol Syst Biol* 4, Page.
30. Halbeisen, R. E., and Gerber, A. P. (2009) Stress-Dependent Coordination of Transcriptome and Translatome in Yeast. *PLoS Biol* 7, Page.
31. Timmermann, B., Jarolim, S., Russmayer, H., Kerick, M., Michel, S., Kruger, A., Bluemlein, K., Laun, P., Grillari, J., Lehrach, H., Breitenbach, M., and Ralser, M. A new dominant peroxiredoxin allele identified by whole-genome re-sequencing of random mutagenized yeast causes oxidant-resistance and premature aging. *Aging (Albany NY)* 2, Page.
32. Tang, H. M., Siu, K. L., Wong, C. M., and Jin, D. Y. (2009) Loss of yeast peroxiredoxin Tsa1p induces genome instability through activation of the DNA damage checkpoint and elevation of dNTP levels. *PLoS Genet* 5, Page.
33. Iraqui, I., Kienda, G., Soeur, J., Faye, G., Baldacci, G., Kolodner, R. D., and Huang, M. E. (2009) Peroxiredoxin Tsa1 is the key peroxidase suppressing genome instability and protecting against cell death in Saccharomyces cerevisiae. *PLoS Genet* 5, Page.
34. Sideri, T. C., Stojanovski, K., Tuite, M. F., and Grant, C. M. Ribosome-associated peroxiredoxins suppress oxidative stress-induced de novo formation of the [PSI+] prion in yeast. *Proc Natl Acad Sci U S A* 107, Page.
35. Lu, P., Vogel, C., Wang, R., Yao, X., and Marcotte, E. M. (2007) Absolute protein expression profiling estimates the relative contributions of transcriptional and translational regulation. *Nat Biotechnol* 25, Page.
36. Alejandro-Osorio, A. L., Huebert, D. J., Porcaro, D. T., Sonntag, M. E., Nillasithanukroh, S., Will, J. L., and Gasch, A. P. (2009) The histone deacetylase Rpd3p is required for transient changes in genomic expression in response to stress. *Genome Biol* 10, Page.
37. Kim, T. S., Liu, C. L., Yassour, M., Holik, J., Friedman, N., Buratowski, S., and Rando, O. J. RNA polymerase mapping during stress responses reveals widespread nonproductive transcription in yeast. *Genome Biol* 11, Page.
38. Vogel, C., de Sousa Abreu, R., Ko, D., Le, S. Y., Shapiro, B., Burns, S. C., Sandhu, D., Boutz, D. R., Marcotte, E. M., and Penalva, L. O. (2010) Sequence signatures and mRNA concentration can explain two-thirds of protein abundance variation in a human cell line. *Molecular Systems Biology* 6, Page.
39. Keller, A., Nesvizhskii, A. I., Kolker, E., and Aebersold, R. (2002) Empirical statistical model to estimate the accuracy of peptide identifications made by MS/MS and database search. *Anal Chem* 74, Page.
40. Nesvizhskii, A. I., Keller, A., Kolker, E., and Aebersold, R. (2003) A statistical model for identifying proteins by tandem mass spectrometry. *Anal Chem* 75, Page.
41. Vogel, C., and Marcotte, E. M. (2008) Calculating absolute and relative protein abundance from mass spectrometry-based protein expression data. *Nat Protoc* 3, Page.
42. Futcher, B., Latter, G. I., Monardo, P., McLaughlin, C. S., and Garrels, J. I. (1999) A sampling of the yeast proteome. *Mol Cell Biol* 19, Page.
43. Eisen, M. B., Spellman, P. T., Brown, P. O., and Botstein, D. (1998) Cluster analysis and display of genome-wide expression patterns. *Proc Natl Acad Sci U S A* 95, Page.
44. Berriz, G. F., King, O. D., Bryant, B., Sander, C., and Roth, F. P. (2003) Characterizing gene sets with FuncAssociate. *Bioinformatics* 19, Page.
45. Hall, M., Frank, E., Holmes, G., Pfahringer, B., Reutemann, P., and Witten, I. H. (2009) The WEKA Data Mining Software: An Update. *SIGKDD Explorations* 11, Page.

46. Bailey, T. L., and Elkan, C. (1994) Fitting a mixture model by expectation maximization to discover motifs in biopolymers. *Proc Int Conf Intell Syst Mol Biol* 2, Page.
47. Pelechano, V., and Perez-Ortin, J. E. There is a steady-state transcriptome in exponentially growing yeast cells. *Yeast* 27, Page.
48. Gsponer, J., Futschik, M. E., Teichmann, S. A., and Babu, M. M. (2008) Tight regulation of unstructured proteins: from transcript synthesis to protein degradation. *Science* 322, Page.
49. Liao, B., Hu, Y., and Brewer, G. (2007) Competitive binding of AUF1 and TIAR to MYC mRNA controls its translation. *Nat Struct Mol Biol* 14, Page.
50. Xue, D., Rubinson, D. A., Pannone, B. K., Yoo, C. J., and Wolin, S. L. (2000) U snRNP assembly in yeast involves the La protein. *Embo J* 19, Page.
51. Pannone, B. K., Xue, D., and Wolin, S. L. (1998) A role for the yeast La protein in U6 snRNP assembly: evidence that the La protein is a molecular chaperone for RNA polymerase III transcripts. *Embo J* 17, Page.
52. Inada, M., and Guthrie, C. (2004) Identification of Lhp1p-associated RNAs by microarray analysis in Saccharomyces cerevisiae reveals association with coding and noncoding RNAs. *Proc Natl Acad Sci U S A* 101, Page.
53. Hasegawa, Y., Irie, K., and Gerber, A. P. (2008) Distinct roles for Khd1p in the localization and expression of bud-localized mRNAs in yeast. *Rna* 14, Page.
54. Hogan, D. J., Riordan, D. P., Gerber, A. P., Herschlag, D., and Brown, P. O. (2008) Diverse RNA-binding proteins interact with functionally related sets of RNAs, suggesting an extensive regulatory system. *PLoS Biol* 6, Page.
55. Godin, K. S., and Varani, G. (2007) How arginine-rich domains coordinate mRNA maturation events. *RNA Biol* 4, Page.
56. Kessler, S. H., and Sachs, A. B. (1998) RNA recognition motif 2 of yeast Pab1p is required for its functional interaction with eukaryotic translation initiation factor 4G. *Mol Cell Biol* 18, Page.
57. Swisher, K. D., and Parker, R. Localization to, and effects of Pbp1, Pbp4, Lsm12, Dhh1, and Pab1 on stress granules in Saccharomyces cerevisiae. *PLoS ONE* 5, Page.
58. Gilbert, W. V., Zhou, K., Butler, T. K., and Doudna, J. A. (2007) Cap-independent translation is required for starvation-induced differentiation in yeast. *Science* 317, Page.
59. Pereira, M. D., Eleutherio, E. C., and Panek, A. D. (2001) Acquisition of tolerance against oxidative damage in Saccharomyces cerevisiae. *BMC Microbiol* 1, Page.
60. Brown, N. M., Torres, A. S., Doan, P. E., and O'Halloran, T. V. (2004) Oxygen and the copper chaperone CCS regulate posttranslational activation of Cu,Zn superoxide dismutase. *Proc Natl Acad Sci U S A* 101, Page.
61. Mannarino, S. C., Vilela, L. F., Brasil, A. A., Aranha, J. N., Moradas-Ferreira, P., Pereira, M. D., Costa, V., and Eleutherio, E. C. Requirement of glutathione for Sod1 activation during lifespan extension. *Yeast*, Page.
62. Terada, T., Oshida, T., Nishimura, M., Maeda, H., Hara, T., Hosomi, S., Mizoguchi, T., and Nishihara, T. (1992) Study on human erythrocyte thioltransferase: comparative characterization with bovine enzyme and its physiological role under oxidative stress. *J Biochem* 111, Page.
63. Ghezzi, P., Romines, B., Fratelli, M., Eberini, I., Gianazza, E., Casagrande, S., Laragione, T., Mengozzi, M., and Herzenberg, L. A. (2002) Protein glutathionylation: coupling and uncoupling of glutathione to protein thiol groups in lymphocytes under oxidative stress and HIV infection. *Mol Immunol* 38, Page.
64. Jun, K. O., Song, C. H., Kim, Y. B., An, J., Oh, J. H., and Choi, S. K. (2009) Activation of translation via reduction by thioredoxin-thioredoxin reductase in Saccharomyces cerevisiae. *FEBS Lett* 583, Page.
65. Porras, P., McDonagh, B., Pedrajas, J. R., Barcena, J. A., and Padilla, C. A. Structure and function of yeast glutaredoxin 2 depend on postranslational processing and are related to subcellular distribution. *Biochim Biophys Acta* 1804, Page.
66. Luikenhuis, S., Perrone, G., Dawes, I. W., and Grant, C. M. (1998) The yeast Saccharomyces cerevisiae contains two glutaredoxin genes that are required for protection against reactive oxygen species. *Mol Biol Cell* 9, Page.
67. Discola, K. F., de Oliveira, M. A., Rosa Cussiol, J. R., Monteiro, G., Barcena, J. A., Porras, P., Padilla, C. A., Guimaraes, B. G., and Netto, L. E. (2009) Structural aspects of the distinct biochemical properties of glutaredoxin 1 and glutaredoxin 2 from Saccharomyces cerevisiae. *J Mol Biol* 385, Page.
68. Grant, C. M., Luikenhuis, S., Beckhouse, A., Soderbergh, M., and Dawes, I. W. (2000) Differential regulation of glutaredoxin gene expression in response to stress conditions in the yeast Saccharomyces cerevisiae. *Biochim Biophys Acta* 1490, Page.
69. Grant, C. M. (2001) Role of the glutathione/glutaredoxin and thioredoxin systems in yeast growth and response to stress conditions. *Mol Microbiol* 39, Page.

70. Kumar, A., Agarwal, S., Heyman, J. A., Matson, S., Heidtman, M., Piccirillo, S., Umansky, L., Drawid, A., Jansen, R., Liu, Y., Cheung, K. H., Miller, P., Gerstein, M., Roeder, G. S., and Snyder, M. (2002) Subcellular localization of the yeast proteome. *Genes Dev* 16, Page.
71. Thorpe, G. W., Fong, C. S., Alic, N., Higgins, V. J., and Dawes, I. W. (2004) Cells have distinct mechanisms to maintain protection against different reactive oxygen species: oxidative-stress-response genes. *Proc Natl Acad Sci U S A* 101, Page.
72. Slekar, K. H., Kosman, D. J., and Culotta, V. C. (1996) The yeast copper/zinc superoxide dismutase and the pentose phosphate pathway play overlapping roles in oxidative stress protection. *J Biol Chem* 271, Page.
73. Ringner, M., and Krogh, M. (2005) Folding free energies of 5'-UTRs impact post-transcriptional regulation on a genomic scale in yeast. *PLoS Comput Biol* 1, Page.
74. Shringarpure, R., and Davies, K. J. (2002) Protein turnover by the proteasome in aging and disease. *Free Radic Biol Med* 32, Page.
75. Shringarpure, R., Grune, T., Mehlhase, J., and Davies, K. J. (2003) Ubiquitin conjugation is not required for the degradation of oxidized proteins by proteasome. *J Biol Chem* 278, Page.
76. Reinheckel, T., Sitte, N., Ullrich, O., Kuckelkorn, U., Davies, K. J., and Grune, T. (1998) Comparative resistance of the 20S and 26S proteasome to oxidative stress. *Biochem J* 335 (Pt 3), Page.
77. Bader, N., and Grune, T. (2006) Protein oxidation and proteolysis. *Biol Chem* 387, Page.
78. Zong, C., Young, G. W., Wang, Y., Lu, H., Deng, N., Drews, O., and Ping, P. (2008) Two-dimensional electrophoresis-based characterization of post-translational modifications of mammalian 20S proteasome complexes. *Proteomics* 8, Page.
79. Demasi, M., Silva, G. M., and Netto, L. E. (2003) 20 S proteasome from Saccharomyces cerevisiae is responsive to redox modifications and is S-glutathionylated. *J Biol Chem* 278, Page.
80. Cuervo, A. M., Palmer, A., Rivett, A. J., and Knecht, E. (1995) Degradation of proteasomes by lysosomes in rat liver. *Eur J Biochem* 227, Page.
81. Tai, H. C., Besche, H., Goldberg, A. L., and Schuman, E. M. (2010) Characterization of the Brain 26S Proteasome and its Interacting Proteins. *Front Mol Neurosci* 3, Page.
82. Ghaemmaghami, S., Huh, W. K., Bower, K., Howson, R. W., Belle, A., Dephoure, N., O'Shea, E. K., and Weissman, J. S. (2003) Global analysis of protein expression in yeast. *Nature* 425, Page.
83. Hieronymus, H., and Silver, P. A. (2003) Genome-wide analysis of RNA-protein interactions illustrates specificity of the mRNA export machinery. *Nat Genet* 33, Page.
84. Hurt, E., Strasser, K., Segref, A., Bailer, S., Schlaich, N., Presutti, C., Tollervey, D., and Jansen, R. (2000) Mex67p mediates nuclear export of a variety of RNA polymerase II transcripts. *J Biol Chem* 275, Page.
85. Gong, Y., Kakihara, Y., Krogan, N., Greenblatt, J., Emili, A., Zhang, Z., and Houry, W. A. (2009) An atlas of chaperone-protein interactions in Saccharomyces cerevisiae: implications to protein folding pathways in the cell. *Mol Syst Biol* 5, Page.
86. Holcik, M., and Sonenberg, N. (2005) Translational control in stress and apoptosis. *Nat Rev Mol Cell Biol* 6, Page.
87. Munhoz, D. C., and Netto, L. E. (2004) Cytosolic thioredoxin peroxidase I and II are important defenses of yeast against organic hydroperoxide insult: catalases and peroxiredoxins cooperate in the decomposition of H2O2 by yeast. *J Biol Chem* 279, Page.
88. Demasi, A. P., Pereira, G. A., and Netto, L. E. (2001) Cytosolic thioredoxin peroxidase I is essential for the antioxidant defense of yeast with dysfunctional mitochondria. *FEBS Lett* 509, Page.
89. Berry, D. B., and Gasch, A. P. (2008) Stress-activated genomic expression changes serve a preparative role for impending stress in yeast. *Mol Biol Cell* 19, Page.
90. Mewes, H. W., Dietmann, S., Frishman, D., Gregory, R., Mannhaupt, G., Mayer, K. F., Munsterkotter, M., Ruepp, A., Spannagl, M., Stumpflen, V., and Rattei, T. (2008) MIPS: analysis and annotation of genome information in 2007. *Nucleic Acids Res* 36, Page.
91. Hieronymus, H., and Silver, P. A. (2004) A systems view of mRNP biology. *Genes Dev* 18, Page.
92. Belle, A., Tanay, A., Bitincka, L., Shamir, R., and O'Shea, E. K. (2006) Quantification of protein half-lives in the budding yeast proteome. *Proc Natl Acad Sci U S A* 103, Page.
93. Rice, P., Longden, I., and Bleasby, A. (2000) EMBOSS: the European Molecular Biology Open Software Suite. *Trends Genet* 16, Page.
94. Linding, R., Jensen, L. J., Diella, F., Bork, P., Gibson, T. J., and Russell, R. B. (2003) Protein disorder prediction: implications for structural proteomics. *Structure* 11, Page.
95. Arava, Y., Boas, F. E., Brown, P. O., and Herschlag, D. (2005) Dissecting eukaryotic translation and its control by ribosome density mapping. *Nucleic Acids Res* 33, Page.
96. Arava, Y., Wang, Y., Storey, J. D., Liu, C. L., Brown, P. O., and Herschlag, D. (2003) Genome-wide analysis of mRNA translation profiles in Saccharomyces cerevisiae. *Proc Natl Acad Sci U S A* 100, Page.
97. Fraser, H. B., Hirsh, A. E., Giaever, G., Kumm, J., and Eisen, M. B. (2004) Noise minimization in eukaryotic gene expression. *PLoS Biol* 2, Page.

98. Wang, Y., Liu, C. L., Storey, J. D., Tibshirani, R. J., Herschlag, D., and Brown, P. O. (2002) Precision and functional specificity in mRNA decay. *Proc Natl Acad Sci U S A* 99, Page.
99. Lawless, C., Pearson, R. D., Selley, J. N., Smirnova, J. B., Grant, C. M., Ashe, M. P., Pavitt, G. D., and Hubbard, S. J. (2009) Upstream sequence elements direct post-transcriptional regulation of gene expression under stress conditions in yeast. *BMC Genomics* 10, Page.
100. Shalgi, R., Lapidot, M., Shamir, R., and Pilpel, Y. (2005) A catalog of stability-associated sequence elements in 3' UTRs of yeast mRNAs. *Genome Biol* 6, Page.
101. Cherry, J. M., Adler, C., Ball, C., Chervitz, S. A., Dwight, S. S., Hester, E. T., Jia, Y., Juvik, G., Roe, T., Schroeder, M., Weng, S., and Botstein, D. (1998) SGD: Saccharomyces Genome Database. *Nucleic Acids Res* 26, Page.
102. Giaever, G., Chu, A. M., Ni, L., Connelly, C., Riles, L., Veronneau, S., Dow, S., Lucau-Danila, A., Anderson, K., Andre, B., Arkin, A. P., Astromoff, A., El-Bakkoury, M., Bangham, R., Benito, R., Brachat, S., Campanaro, S., Curtiss, M., Davis, K., Deutschbauer, A., Entian, K. D., Flaherty, P., Foury, F., Garfinkel, D. J., Gerstein, M., Gotte, D., Guldener, U., Hegemann, J. H., Hempel, S., Herman, Z., Jaramillo, D. F., Kelly, D. E., Kelly, S. L., Kotter, P., LaBonte, D., Lamb, D. C., Lan, N., Liang, H., Liao, H., Liu, L., Luo, C., Lussier, M., Mao, R., Menard, P., Ooi, S. L., Revuelta, J. L., Roberts, C. J., Rose, M., Ross-Macdonald, P., Scherens, B., Schimmack, G., Shafer, B., Shoemaker, D. D., Sookhai-Mahadeo, S., Storms, R. K., Strathern, J. N., Valle, G., Voet, M., Volckaert, G., Wang, C. Y., Ward, T. R., Wilhelmy, J., Winzeler, E. A., Yang, Y., Yen, G., Youngman, E., Yu, K., Bussey, H., Boeke, J. D., Snyder, M., Philippsen, P., Davis, R. W., and Johnston, M. (2002) Functional profiling of the Saccharomyces cerevisiae genome. *Nature* 418, Page.
103. Kertesz, M., Wan, Y., Mazor, E., Rinn, J. L., Nutter, R. C., Chang, H. Y., and Segal, E. (2010) Genome-wide measurement of RNA secondary structure in yeast. *Nature* 467, Page.